Design of the Retarding Potential Analyzer to be used with BURFIT-80 Ion Thruster and Validation using PIC-DSMC Code

Mert Satir*, Fırat Sik, Emre Turkoz, Murat Celik
Department of Mechanical Engineering
Bogazici University
Istanbul, Turkey
*Corresponding Author: mertsatir@gmail.com

***Abstract*—For better integration of plasma thrusters into spacecraft and satellites, potential damaging effects of impinging high energy ions on the spacecraft surfaces should be taken into consideration. For analyzing the plume plasma in this regard, retarding potential analyzers (RPA) are used in electric propulsion as one of the most fundamental and widely used diagnostics tools. RPA determines the ion energy distribution of plume plasma which is in the downstream of a thruster. This paper reports on a successful design process of an RPA to be used with BURFIT-80 ion thruster. An in-house developed hybrid Particle-In-Cell Direct Simulation Monte Carlo (PIC-DSMC) code, which is previously applied for ion thruster grid region is implemented to simulate the flow in the RPA. Results are used to validate the effective operation of the RPA. Potential distributions in the RPA are investigated and the calculated currents collected by the collector is compared with an existing experimental study.**

Keywords— electric propulsion, plasma diagnostics, retarding potential analyzer, plasma simulations.

I. INTRODUCTION

The need for analyzing the processes behind the electric propulsion became important and necessary with the developing thruster performance capabilities. Characterizing the plume plasma is essential to have a comprehensive idea about the performance, efficiency, thrust parameters and determining possible plume interactions with the components of the spacecraft and satellites. As a result of the electric thrusters' plume plasma impingements on sensitive surfaces such as solar arrays, severe damages on these components occur by sputtering. In order to determine the interaction between the impinging plume particles and the spacecraft surfaces, the ion and electron transport properties must be defined in terms of the spatial location around the spacecraft. Therefore, perturbing measurements are done in order to examine the parameters of the plume plasma.

Numerous probes are available for plume diagnostics due to incapability of a single probe to determine all plume parameters. The retarding potential analyzer (RPA) is one of those diagnostics devices which is designed for measuring the ion energy distribution at the plume. Used with the ion current density, this information provides the knowledge about the thrust and the lifetime of the spacecraft and satellites.

II. WORKING PRINCIPLE

An RPA consists of a current collector and a set of biased grids as seen in Fig.1. It collects the selectively filtered ions above a set limit energy by applying an ion retarding grid potential [1]. Plume plasma coming from the plasma source enters into device and passes through a set of grids, and reaches to current collecting surface. The probe filters the plume constituents and allows only ions with the energies greater than the energy corresponding to the set grid voltage to reach the current collector. In other words, it removes all the electrons from the plume and selectively repels the ions that has energy ε_i or voltage value ($V = \varepsilon_i / e$ where e is the elementary charge) less than the ion retarding voltage. By the use of a retarding electrostatic potential, RPA derives the kinetic energy of the particles from the height of the corresponding potential barrier that particles can overcome.

RPAs in general have mainly four grids [1]. The first grid is a floating grid used for reducing the plasma perturbation and attenuate the density in the RPA. The second one, electron repelling grid is negatively biased for repelling the electrons. It is biased to a sufficiently negative voltage, so none of the electrons can pass that grid. The third one is the ion retarding grid which is positively biased at various high values by sweeping the voltage from 0 V. At each bias voltage value, only ions that have higher energy than the imposed voltage by the grid can pass. The fourth one, secondary electron repeller grid may be used in order to prevent the errors due to the secondary electron emission (SEE) phenomena. When the ions with the sufficient energy hit on the current collector, they have a chance to induce the emission of secondary electrons from that surface. Secondary electron repeller grid is negatively biased compared to the collector, so the emitted secondary electrons from the collector will return to it. Since the flux of incoming ions and the flux of the emitted secondary electrons can not be distinguished by the ammeter, these secondary electrons should be added back to collected current. And lastly, the ion collector is either

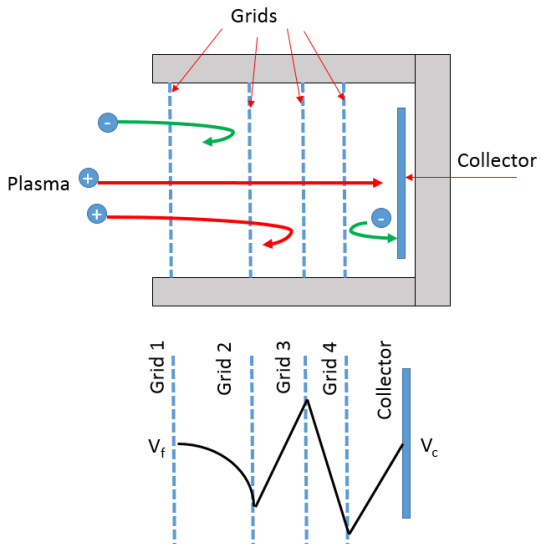

Fig. 1. Schematic of an RPA and bias voltages applied to grids

grounded or slightly negatively biased to attract the ions. So the current can be measured by the incoming ions.

For measuring the ion energy distribution function, the collector current should be recorded as a function of the retarding grid potential. By taking the first derivative of the resultant collector current with respect to the ion retarding grid potential, ion energy distribution can be obtained [2]. It is given by;

$$-\frac{dI}{dV} = \frac{A_c q_i^{\,2} n_i e^2}{m_i} f(V) \qquad (1)$$

where A_c is the probe collection area, q_i is the charge-state of the ion, n_i is the ion density, e is the elementary charge and m_i is the ion mass [3]. Equation (1) indicates that the negative derivative is proportional to the Ion Voltage Distribution Function (IEDF), $f(\varepsilon_i)$. Since voltage $V = \varepsilon_i / e$, ion energy distribution function can be deduced from the function $f(V) = f(\varepsilon_i / e)$.

One drawback of the RPA is that it does not discriminate between singly charged and multiply charged ions. RPA can only measure the ion energy distribution as if the plasma is composed of same species of ions which have same mass and charge [4]. Filtration of RPA is not done based on the ion energy, but rather the ion energy per unit charge. Therefore a Xe^+ ion that has energy of 250 eV and a Xe^{2+} ion that has energy of 500 eV will not be differentiated by RPA. Therefore, in data reduction of RPA measurements, all collected ions are assumed to be singly charged. However, electric thrusters' plumes do not only have singly charged ions but also multiply charged ions. Measurement results by an ExB probe on the Xenon Hall thruster plume for various discharge voltages showed that plume may be composed of up to 12% Xe^{2+} and 2% Xe^{3+} other than singly charged Xe^+ ions [5]. For RF-ion thrusters, singly charged xenon ions are identified as the main component of the ion beam. The fraction of doubly charged ions is below 1% [6].

III. DESIGN

Design of an RPA should be completed depending on the specific application. Although RPA probe is well documented and widely applied to various electric propulsion systems, their design is not straightforward due to their accuracy of low and high energetic ion transmission. In the literature about RPA, the focus is on Hall thrusters [7], [8], [9], [10]. The theory of the plume diagnostics of different electric propulsion systems are similar, however the plume characteristic are different. Consequently the design parameters of the RPA may vary, that means design of the RPA requires a parametric study. Taking the design parameters and limits into consideration, an RPA design can be applied to any thruster type. The limitations should be considered carefully and designed for proper values.

For RPA design to be used in the RF ion thruster BURFIT-80 [11] which is designed at the Bogazici University Space Technologies Laboratory (BUST-Lab), relevant, similar thruster plume characterizations are investigated such as RIT-10, RIT-15, NSTAR etc., since the design of the BURFIT-80 is inspired by these thrusters. With its beam voltage and current, RIT-10 is the most similar thruster to BURFIT-80. So required data for designing the RPA are obtained from RIT-10 studies [12], [13]. It is designed to operate at 100 mm – 1000 mm axial distance on the thruster exit centerline where the electron temperature and the electron density are approximated as 1.8 eV and $1x10^{17}$ m^{-3} respectively. Since these parameters are unknown in the RPA probe, it is estimated that the plume parameters are valid for inside of the RPA [7].

RPA covers the grids and collector in a stainless steel casing as seen in Fig.2 which is grounded to vacuum tank potential. All the information about the parts of the RPA is given in Table II. The casing has an outer diameter of 12.7 mm, an inner diameter of 10.7 mm and a length of 38 mm. The entrance aperture of the outer casing is 6.5 mm. Inside the casing, an electrical insulator inner sleeve is used in order to insulate the grids and the current collector from the casing.

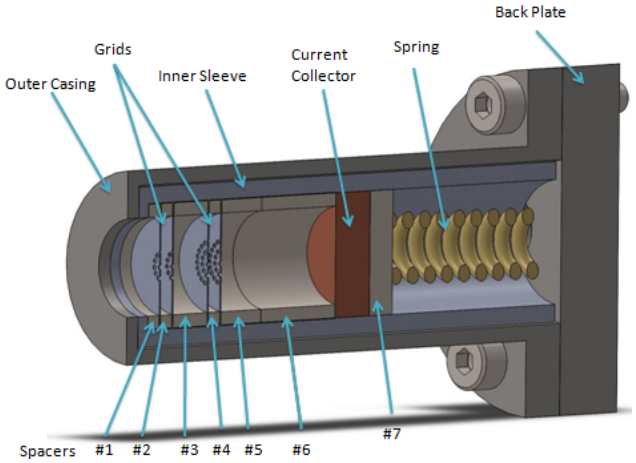

Fig. 2. 3D cross-sectional view of the RPA

TABLE I. DIMENSIONS OF THE MACOR WASHERS

Washer #	1	2	3	4	5	6	7
Thickness	1 mm	1 mm	3 mm	1 mm	3.5 mm	6.5 mm	2 mm

The inner sleeve is made of boron nitride which is a good electrical insulator and has an outer diameter of 10.5 mm and an inner diameter of 8.8 mm, and a length of 36.5 mm. The collector plate is placed about 18 mm downstream of the aperture, so it enables a collimation angle of 20°. This ensures that ions which are coming only from near the exit plane of the thruster are collected. This should be guaranteed not to measure low energy ions that encountered CEX collisions.

The grids and collector are separated by MACOR spacers thanks to its low thermal conductivity and excellent electrical properties. Each MACOR washer is machined to the correct thickness in order to provide proper spacing. They have 8.3 mm outer diameter and 6.5 mm inner diameter. Thickness values of the washers can be seen in Table I.

A spring placed behind the rear face of the collector enables the grids and collector to be linked to the back cover of the RPA. Back cover is screwed to the outer casing with a socket head cap screw and a hex nut. 0.1 mm molybdenum electrical wire connections are made by spot welding them to the grids and they are aligned between the sleeve's outer edge and inner edge of the casing and exiting at the back of the probe.

A. Grid Design

Debye length is a critical parameter for the operation of the RPA. The spacing of electron repelling and ion retarding grids and the aperture size on the grids are directly proportional to the Debye length. According to the analyzer design of Hutchinson [1], the grid apertures should be less than the thickness of the sheath in order to minimize the shielding effect of the grids by the plasma. As suggested by [7], the grid aperture should be around two Debye length.

TABLE II. INFORMATION ABOUT THE RPA PARTS

Part	**Material**	**Size**		
Outer Casing	316 SS	O.D. 12.7 mm	I.D. 10.7 mm	Length 38 mm
Inner Sleeve	Boron Nitride	O.D. 10.5 mm	I.D. 8.8 mm	Length 36.5 mm
Washers	MACOR	O.D. 8 mm	I.D. 6.5 mm	
Grids	Molybdenum	O.D. 8 mm	Thickness 0.1 mm	
Collector	Copper	O.D. 10.5 mm	Thickness 3 mm	
Electrical Wires	Molybdenum	38 AWG (0.1 mm)		

Another important consideration on the RPA design is the space charge effect. Charge density between the grids is able to develop a potential hill and the ion retarding potential may be altered to a higher value than the applied potential. Consequently, it will cause erroneous current collection. Hutchinson [1] derived a relation by equating the ion Bohm flux to Child Langmuir flux as;

$$\frac{x}{\lambda_D} = 1.02\left(\frac{eV}{kT_e}\right)^{\frac{3}{4}} \tag{2}$$

where x is the grid spacing, λ_D is the Debye length, e is the elementary charge and V is the potential between the grids at which space charge effects are greatest. It is maximum when the sweeping grid is set to 0 V that will allow all the ions to pass through the ion retarding grid. Hutchinson suggests that for repelling all incoming electrons, potential applied on the electron retarding grid should be a few times T_e. Thus, the distance between electron and ion retarding grids should be less than 4 λ_D to avoid space charge effect. This consideration is especially significant in the gap between the electron and ion retarding grids because the space charge effect would most likely exist in that region.

Considering the approximated electron temperature and density values for BURFIT-80, calculated Debye length is around 0.04 mm. We are able to photochemically etch the grids with 0.08 mm (2 times Debye length) diameter apertures however carrying out the space charge effect criteria which suggests the grid spacing should be less than four Debye length is out of our manufacturing capabilities. For high density plasmas in which the Debye length is short, the criteria of space charge effect avoidance becomes too difficult to satisfy. So this leads to both a small grid spacing and a small volume capable of inducing an arc discharge. The grids spaced only microns apart would lead to possible arcing phenomena. Also, the manufacturing and assembly of grids would not be feasible in such microscopic tolerances. So in our case, grids closer than 0.16 mm which is $4\lambda_D$ would be hard to maintain.

As indicated by Hutchinson, the Debye length of the plasma incident to the RPA can be increased by means of a low transparency mesh. Thus an entrance floating grid that has low transparency provides attenuation of the plasma flux before it encounters the electron repelling grid and this leads to reduce the number density and increase the Debye length inside the probe. Maximum allowable, limiting density at the electron repeller grid can be calculated by the Green's relation [14]. It is expressed as;

$$n \le \frac{4}{9}\frac{\varepsilon_0 E_i}{e^2 x^2} \tag{3}$$

where x is the grid spacing and E_i is the minimum kinetic energy for the ions at the electron repeller grid, ε_0 is the permittivity of free space and e is the elementary charge.

Setting the feasible grid spacing to 1 mm in (3); the attenuation that the entrance grid should implement is calculated. In our case, density should be attenuated at least 42 times in order to prevent space charge effects in the region of highest density. So double entrance grid is designed. The first and second grids are designed to have a transmission of 10% and 20% respectively.

Due to collisions with the grid, the density outside of the electron repeller grid will be reduced by the attenuation factor of 50 and the electron density will be $n_e = 2x10^{15}$ m^{-3} The new Debye length with the reduced density is increased to 0.28 mm. Accordingly this will relax the requirement for grid aperture size. So 0.3 mm which is less then $2\lambda_D$ is chosen easily for the aperture diameter. With the reduced density and the corresponding increased Debye length, aforementioned two criteria are satisfied:

- Grid apertures are 0.3 mm and this size fulfills the minimization of the shielding effect of the grids by the plasma since it is less than two Debye length. Thus the intended repelling of the electrons and ions by the grids will be successfully achieved.
- The spacing between the electron repeller and the ion retarding grids is 1 mm and the space charge effects between these grids are prevented since this size is less then four Debye length.

The electron repeller and ion retarding grids will have 40% transparency. The thickness of the grids will be 0.1 mm according to existing designs [15], [8]. The grid material is molybdenum due to its low secondary electron emission yield [16]. Grids are 8 mm diameter round foils. The collector is a copper disc. Fortunately, for impact energies below 1 keV, SEE yield of copper is less than 0.1 electrons per ion [17] and the potential source of error due to secondary electron current is thought to be negligible since the expected SEE yield from the copper collector can be considered low. This is supported by RPA tests, which included the electron suppression grid on the upstream of the collector (between washers 5 and 6 in Fig.2). Tests with and without the secondary electron suppression grid yielded no noticeable change in the collected current [9].

Considering the low electron emission from the collector and the molybdenum grids, in this presented study, the secondary electron suppression grid is neglected in order to maximize the open area fraction of the grid system and ensure an adequate signal to noise ratio. The same reasoning is applied in Azziz's study [10] which uses a stainless steel collector in the RPA. It is stated that the secondary electron emission in the RPA from ion bombardment of the stainless steel surfaces not a concern since the secondary electron yield due to Xe^+ bombardment at energies below 1 keV is less than 0.02 electrons per ion [16].

IV. VALIDATION OF RPA WITH PIC CODE

RPA design in this study should be ensured to work efficiently. In the uncertainty analysis of the RPA, ion optics of the grids should be inspected. Depending on the grid thickness, applied grid potentials may differ in the center of the grid apertures. It may result in an *effective potential* lower than the actual bias at these points. Therefore, collected ions will be detected at incorrectly higher energies. A thick ion retarding grid should be used in order to minimize these lower potential points in the grid apertures or this minimization can be done by employing two ion retarding grids separated by an insulator [18].

In Marrese's study [7], the required grid thickness is found by the PIC code MAGIC to ensure the effective decelerating potential of the ion retarding grid is greater than 98% of the applied voltage considering that it is a sufficient percentage. In another study by Sullivan [19], with the help of a program called Simion, electrostatic potential distribution in the RPA is calculated, and the results showed that there exist a 2-3% of the applied retarding voltage drop in the center of grid apertures. In Spirkin's study [20], the flow inside an RPA is simulated by a PIC code and the collected current by the collector is estimated.

Our RPA design is validated by the PIC-DSMC code [21], [22] which is developed at BUST-Lab specifically for simulating the physics of ion optics in the intra-grid region at the end of the discharge chamber of an ion thruster which is benefited from the study of Farnell [23] and Nakayama [24]. It is a 2D-axisymmetric, second order finite difference, time dependent code that simulates the ion and neutral flow through the grid apertures. Electric potentials are calculated by solving the Poisson's equation in cylindrical coordinates. Thus, ion particle motions through the grid apertures can be performed by applying the Lorentz force depending on the electric field along the domain. The solution domain is a 30^o slice.

For validating the designed RPA, experimental data from Azziz's study [10] is used for the inlet data of the code. Ion drift velocity is calculated from the RPA measurement of most probable ion energy in the plume of the Hall thruster operating at 300 V discharge voltage. As stated in the study, the most probable energy is 260 eV at 1 m downstream from the exit plane for the 300 V operating condition. From the conservation of energy, we calculated the most probable velocity as 19548 m/s. The ions enter the RPA with a Maxwellian distribution around this velocity. The approximated ion density in Azziz's study at 1 m downstream from the exit plane is $n_i = 6x10^{14}$ m^{-3}. After passing through the attenuating grids, ion density becomes $n_i = 1.2x10^{13}$ m^{-3}. Electron repeller grid is set to -30 V which is around 15 times T_e. As stated by Hutchinson -30 V is enough to repel all the electrons entering the probe [1].

The computational domain employed in the code is 700x50 mesh which is 14.2 mm in length and 0.25 mm in diameter as seen in Fig.3. 14.2 mm represents the distance from the second floating grid to the collector. The code is used to validate the effectiveness of the grid thickness values as suggested by Marrese [7] with the determined aperture size and grid spacing as as suggested by Hutchinson [1].

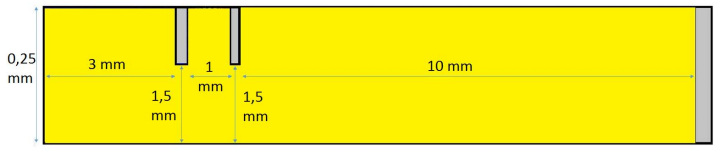

Fig. 3. The solution domain for the code cross-sectional view of the RPA

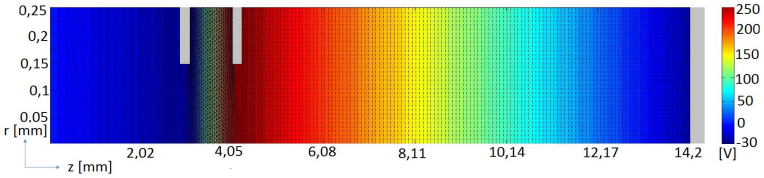

Fig. 4. Equipotentials in RPA after some time ($V_{ion\ retarding}$ = 250 V and $V_{electron\ repeller}$= -30 V)

In Table III, it is shown that that the effective potentials of the ion retarding grid is greater than 98% of the applied potentials. One can see that the effective potentials are weakened by the other grids due to RPA's small dimensions (close-spaced configuration).

Fig.4 shows that space charge limitation is avoided between the grids. A potential hill which is higher than the applied potential due to the presence of space charge does not occur.

The original code simulates only the ions and neutrals since there are no electrons between the thruster grid region. So implementing this code into RPA simulation after the electron repelling grid is valid since it is assumed that there are no electrons after that grid considering the Hutchinson's suggestion [1].

The electron repeller grid is set to -30 V and ion retarding grid is swept from 0 V to 400 V. The collected currents for various ion retarding potentials are recorded and compared with the experimental results obtained in [10]. The numerical timestep which the currents are collected at is determined considering the time of flight that ions entering the RPA at the highest velocity reach the collector. However, the ions have a Maxwellian velocity distribution. Accordingly it is assumed that collecting the current at the corresponding timestep of 20 times the time of flight will guarantee that all the ions are collected including the ones at the lower tail of the Maxwellian distribution. It is seen in Fig.5 and Fig.6 that the obtained results are similar to the experimental data in Azziz's study as expected.

TABLE III. APPLIED AND EFFECTIVE POTENTIALS ON GRIDS

$V_{ion\ retarding}$		$V_{electron\ repeller}$	
Applied	**Effective**	**Applied**	**Effective**
400 V	395 V	-30 V	-25 V
300 V	295 V	-30 V	-26 V
200 V	196 V	-30 V	-27 V
100 V	98 V	-30 V	-27 V
0 V	0 V	-30 V	-27 V

V. CONCLUSION AND FURUTE WORK

A retarding potential analyzer to be used in ion energy distribution measurements of the BURFIT-80 RF ion thruster is designed. The design considerations are investigated carefully.

RPA is an intrusive diagnostics tool. Therefore keeping the size small is crucial for RPA. However small sizing brings some drawbacks such as weak ion current signal strength, space charge limitation, possible arcing phenomena or lower potential points than the applied potentials at the center of the grid apertures.

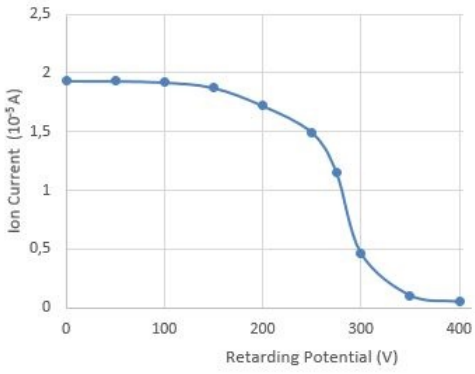

Fig. 5. Obtained current versus ion retarding potential with the PIC code simulating the 300 V discharge voltage Hall thruster

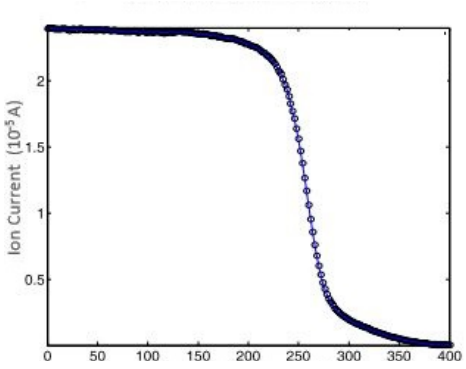

Fig. 6. Measured current versus ion retarding potentail with the RPA in Azziz's study for a 300 V discharge voltage Hall thruster [10]

Design of the RPA is aided by a 3D PIC code and it is ensured that RPA works properly. Space charge limitation is not observed between the grids. With the determined grid thickness, it is shown that the potentials calculated at the aperture centers are 98% of the applied potential and lastly expected ion currents are obtained similar to the experimental results.

As the future work, ion energy distribution measurements will be conducted after the BURFIT-80 is built and the results will be compared to the existing studies. Possible broadening effects in the distributions and other possible uncertainties in the RPA measurement results will be explained.

Acknowledgment

The research is financially supported by Turkish Scientific and Technological Research Council (TUBITAK) under project numbers 112M862, 113M244 and partially by Bogazici University Scientific Research Projects Office (BAP) under project numbers BAP-6184 and BAP-8960.

References

[1] Hutchinson, I. H., Principles of Plasma Diagnostics," Cambridge University Press, 2002.

[2] Bohm, C. and Perrin, J., "Retarding-Field Analyzer for Measurements of Ion Energy Distributions and Secondary Electron Emission Coefficients in Low-Pressure Radio Frequency Discharges," Review of Scientific Instruments, Vol. 64, No. 1, 1993, pp. 31–44.

[3] King, L. B., "Transport-Property and Mass Spectral Measurements in the Plasma Exhaust Plume of a Hall-Effect Space Propulsion System," Ph.D. Thesis, The University of Michigan, Ann Arbor, MI, USA, 1998.

[4] Prioul, M., Bouchoule, A., Roche, S., Magne, L., Pagnon, D., Touzeau, M., and Lasgorceix, P., "Insights on Physics of Hall Thrusters Through Fast Current Interruptions and Discharge Transients," 27th International Electric Propulsion Conference, Pasadena, CA, US, October 2001, IEPC-01-059.

[5] Hofer, R. R. and Gallimore, A. D., "Ion Species Fractions in the Far-Field Plume of a High-Specific Impulse Hall Thruster," 39th Joint Propulsion Conference, Huntsville, AL, USA, July 2003, AIAA-2003-5001.

[6] Zeuner, M., Scholze, F., Tartz, M., Neumann, H., Leiter, H., and Kukies, R., "Ion Beam Characterisation of the RIT 10 Ion Thruster," 39th Joint Propulsion Conference, Huntsville, AL, USA, July 2003, AIAA-2003-5009.

[7] Marrese, C. M., Majumdar, N., Haas, J., Williams, G., King, L., and Gallimore, A. D., "Development of a Single-Orifice Retarding Potential Analyzer for Hall Thruster Plume Characterization," 25th International Electric Propulsion Conference, Cleveland, OH, USA, 1997, IEPC-97-066.

[8] Hofer, R. and Haas, J., "Ion Voltage Diagnositcs in the Far-Field Plume of a High-Specific Impulse Hall Thruster," 39th Joint Propulsion Conference, Huntsville, AL, USA, July 2003, AIAA-2003-4556.

[9] Beal, B. E., Clustering of Hall effect Thrusters for High-power Electric Propulsion Applications, Ph.D. Thesis,The University of Michigan, Ann Arbor, MI, USA, 2004.

[10] Azziz, Y., Experimental and Theoretical Characterization of a Hall Thruster Plume, Ph.D. Thesis, Massachusetts Institute of Technology, Cambridge, MA, USA, 2007.

[11] Yavuz, B., Turkoz, E., and Celik, M., "Prototype Design and Manufacturing Method of an 8 cm Diameter RF Ion Thruster," 6th International Conference on Recent Advances in Space Technologies (RAST), Istanbul, Turkey, June 2013, IEEE.

[12] Winter, M. W., Eichhorn, C., Auweter-Kurtz, M., and Pfrommer, T., "Status on Plasma Diagnostic Measurements on a RIT-10 Ion Thruster," 30th International Electric Propulsion Conference, Florence, Italy, September 2007, IEPC-2007-173

[13] Freisinger, J., Walther, R., and Schaefer, M., "Plasma Diagnostics of the RF-Ion Thruster RIT-10," 9th International Electric Propulsion Conference, Bethesda, MD, USA, April 1972.

[14] Green, T., "Space Charge Effects in Plasma Particle Analyzers," Plasma Physics, Vol. 12, No. 11, 1970, pp. 877.

[15] Linnell, J. A., "An Evaluation of Krypton Propellant in Hall Thrusters," Ph.D. Thesis, The University of Michigan, Ann Arbor, MI, USA, 2007.

[16] Carlston, C., Magnuson, G., Mahadevan, P., and Harrison Jr, D., Electron Ejection from Single Crystals Due to 1-to 10-keV Noble-Gas IonBombardment," Physical Review, Vol. 139, No. 3A, 1965, pp. A729.

[17] Kaminsky, M., Atomic and Ionic Impact Phenomena on Metal Surfaces, Vol. 15, Springer-Verlag Berlin, 1965.

[18] Partridge, J. M., Development and Implementation of Diagnostics for Unsteady Small-Scale Plasma Plumes, Ph.D. Thesis, Worcester Polytechnic Institute, Worcester, MA, USA, 2009.

[19] Sullivan, R. M., The Physics of High-Velocity Ions in the Hall Thruster Near-Field, Ph.D. Thesis, California Institute of Technology, Pasadena, CA, USA, 2010.

[20] Spirkin, A. and Gatsonis, N. A., "Unstructured 3D PIC Simulations of the Flow in a Retarding Potential Analyzer," Computer physics communications, Vol. 164, No. 1, 2004, pp. 383–389.

[21] Turkoz, E., Sik, F., and Celik, M., "A Study of Ion Thruster Optics through Particle Simulations and Evaluation of the Near Plume Plasma Properties," 50th Joint Propulsion Conference, July 2014, AIAA-2014-3412.

[22] Turkoz, E., Sik, F., and Celik, M., "Trajectory Studies through Numerical Simulation of Ion Thruster Grid Region Plasma with PIC-DSMC Approach in 3D," 5th Russian-German Conference on Electric Propulsion, September 2014.

[23] Farnell, C. C., Performance and Lifetime Simulation of Ion Thruster Optics, Ph.D. Thesis, Colorado State University, Fort Collins, CO, USA, 2007.

[24] Nakayama, Y. and Wilbur, P. J., "Numerical Simulation of High Specific Impulse Ion Thruster Optics," 27th International Electric Propulsion Conference, October 2001, IEPC-01-099.